Proc. Natl. Acad. Sci. USA
Vol. 95, pp. 328–333, January 1998
Neurobiology

Null mutation in the rhodopsin kinase gene slows recovery kinetics of rod and cone phototransduction in man

(dark adaptation/nightblindness/Oguchi disease/photoreceptor/retina)

ARTUR V. CIDECIYAN[†‡], XINYU ZHAO[§¶], LORI NIELSEN[‖], SHAHROKH C. KHANI[‖**], SAMUEL G. JACOBSON[†], AND KRZYSZTOF PALCZEWSKI[§¶]

[†]Department of Ophthalmology, Scheie Eye Institute, University of Pennsylvania, Philadelphia, PA 19104; Departments of [§]Ophthalmology and [¶]Pharmacology, University of Washington, Seattle, WA 98195; and Departments of [‖]Ophthalmology and [**]Biochemistry, State University of New York, Buffalo, NY 14215

Edited by Jeremy Nathans, Johns Hopkins University School of Medicine, Baltimore, MD, and approved October 31, 1997 (received for review September 12, 1997)

ABSTRACT **Rhodopsin kinase (RK), a specialized G-protein-coupled receptor kinase expressed in retina, is involved in quenching of light-induced signal transduction in photoreceptors. The role of RK in recovery after photoactivation has been explored *in vitro* and *in vivo* experimentally but has not been specifically defined in humans. We investigated the effects on human vision of a mutation in the RK gene causing Oguchi disease, a recessively inherited retinopathy. *In vitro* experiments demonstrated that the mutation, a deletion of exon 5, abolishes the enzymatic activity of RK and is likely a null. Both a homozygote and heterozygote with this RK mutation had recovery phase abnormalities of rod-isolated photoresponses by electroretinography (ERG); photoactivation was normal. Kinetics of rod bleaching adaptation by psychophysics were dramatically slowed in the homozygote but normal final thresholds were attained. Light adaptation was normal at low backgrounds but became abnormal at higher backgrounds. A slight slowing of cone deactivation kinetics in the homozygote was detected by ERG. Cone bleaching adaptation and background adaptation were normal. In this human *in vivo* condition without a functional RK and probable lack of phosphorylation and arrestin binding to activated rhodopsin, reduction of photolyzed chromophore and regeneration processes with 11-*cis*-retinal probably constitute the sole pathway for recovery of rod sensitivity. The role of RK in rods would thus be to accelerate inactivation of activated rhodopsin molecules that in concert with regeneration leads to the normal rate of recovery of sensitivity. Cones may rely mainly on regeneration for the inactivation of photolyzed visual pigment, but RK also contributes to cone recovery.**

When light is absorbed in the retinal photoreceptors by visual pigments, these molecules are transformed from quiescent to a catalytically active form capable of activating hundreds of G protein molecules. A cascade of biochemical reactions ensues resulting in an electrophysiological signal and vision (1). Recovery after photoactivation occurs rapidly in readiness for further light stimuli. The activated form of the rod visual pigment rhodopsin, for example, is inactivated by multiple steps including: phosphorylation by rhodopsin kinase (RK) and binding of a regulatory protein arrestin, removal and reduction of photolyzed chromophore all-trans-retinal by retinol dehydrogenase, and finally the complete inactivation that is accomplished by dephosphorylation and regeneration of rhodopsin with 11-*cis*-retinal. Parallel steps take place in the recovery of photolyzed species of cone visual pigments, but the kinetics are faster (2).

Much has been learned about the recovery mechanisms following photoactivation from biochemical reconstitution systems (3), but the physiologic importance of these pathways in human vision remains to be defined. Whereas it is usually basic science that increases our understanding of human retinal disease, there are occasional opportunities when the study of human retinopathy can help elucidate fundamental retinal processes as they relate to humans. Such an opportunity presented recently in Oguchi disease, an autosomal recessive condition in which patients experience night blindness caused by a markedly prolonged insensitivity of their rod vision after light exposure (4). Two genes, both encoding photoreceptor proteins involved in recovery after photoactivation, have been found to be mutated in Oguchi disease (5, 6). Arrestin mutations were first discovered to be disease-causing in Oguchi patients of Japanese origin (5). More recently, the RK gene was implicated in Oguchi patients of European ancestry (6). RK is one of the most specialized of a family of serine/threonine kinases involved in desensitization of G protein-coupled receptors (7). In the Oguchi patients, a point mutation in the catalytic region, a deletion in the C terminus, and a deletion of exon 5 were identified in the RK gene (6).

The present work seeks to understand the role of RK in human vision through study of Oguchi disease caused by an exon 5 deletion in the RK gene.

MATERIALS AND METHODS

PCR Amplification of the RK Gene from Patient DNA. Genomic DNA was isolated from blood of the patient and his relatives (Pharmacia), and PCR reaction was carried out as described (8). The primers used are: exon 5-exon 6, XZ-57 (5′-GACTTCTCCGTGGACTACTTTGC-3′) and XZ-54 (5′G-CCTCCAGCTGCCTCCAGTTAAG-3′); deletion junction, XZ-59 (sense primer for deletion junction: 5′-CAGGGCCAG-TGGTCGAAGGTCTCAA-3′, ref. 6) and XZ-56 (antisense primer for deletion junction: CTGTCCTGGCAGGACAGTC-ACATGT-3′, ref. 6); deletion junction-exon 6, XZ-59 and XZ-54; and exon 6-exon 7, XZ-49 and XZ-46B. Plasmid DNA containing exon 4–7 of human RK (provided by T. Dryja, Harvard University) was used as a positive control template in PCR reactions.

Heterologous Expression of Wild-Type and the Deletion Mutant of RK in COS-7 Cells. The eukaryotic expression plasmid pCMV-HRK encoding wild-type human RK was constructed by ligating *Hin*dIII-*Xba*I digested pCMV5 vector (9) to a *Hin*dIII-*Nhe*I cDNA cassette containing the coding wild-type RK cDNA sequence flanked by 33 bases of 5′- and 85 bases of 3′-untranslated sequences. The plasmid pCMV-HRK(X5 del) encoding the mutant form was constructed by ligating digested pCMV5 with an analogous mutant *Hin*dIII-*Nhe*I cDNA cassette containing RK sequence lacking in exon

The publication costs of this article were defrayed in part by page charge payment. This article must therefore be hereby marked "*advertisement*" in accordance with 18 U.S.C. §1734 solely to indicate this fact.

This paper was submitted directly (Track II) to the *Proceedings* office.
Abbreviations: RK, rhodopsin kinase; Rho*, activated form of rhodopsin; ERG, electroretinograph(y); ISI, interstimulus interval.
‡To whom reprint requests should be addressed at: Scheie Eye Institute, 51 North 39th Street, Philadelphia, PA 19104. e-mail: cideciya@mail.med.upenn.edu.

5. The mutant *Hin*dIII-*Nhe*I cDNA cassette was generated from the wild-type RK cDNA in Bluescribe (Stratagene) by a combination of standard techniques including site-directed mutagenesis on double-stranded template using QuickChange kit (Stratagene). The wild-type sequences immediately surrounding the proximal and distal junction of exon 5 were converted to *Stu*I and *Pml*I sites, respectively, on the cDNA in two sequential mutagenesis steps using the mutagenic oligonucleotides, 5′-GGGACCCCAGGCCTCATGGCCCCCGAGCTCC-3′ (codon 354–363), and 5′-CCGTGGAGAGCACGTGGAGAACAAGGAGCTG-3′ (codon 395–404) as primers in *Pfu* polymerase reaction. The resultant DNA was then digested with *Pml*I and *Stu*I and religated to excise the *Pml*I-*Stu*I fragment corresponding nearly to the entire sequence of exon 5 from the cDNA. Finally, oligonucleotide 5′-CTACGCAGGGACCCCAGGTGGAGAACAAGG-3′ was used in a site-directed mutagenesis reaction to delete a single remaining junctional nucleotide from the religated cDNA to generate the mutant cassette for construction of pCMV-HRK(X5 del). Alterations in the sequences were verified by DNA sequencing. The expression plasmids were transfected into subconfluent monolayers of COS-7 cells in the presence of DEAE dextran by standard techniques (9). The cells were harvested 48 hr after transfection, lysed, and transfected COS-7 supernatants were assayed for RK activity within 6 hr of preparation in the presence of 30 μM benzamidine to minimize proteolysis (10).

Psychophysics. Dark- and light-adapted static threshold perimetry, bleaching, and background adaptation were performed (11). For bleaching adaptation, monochromatic stimuli (500, 650 nm) were tested at 12° in the inferior field (12). Prebleach baseline dark-adapted (>10 hr for homozygote, >3 hr for heterozygote) thresholds were established. Full (99%) and partial (2%) bleaches were delivered and thresholds determined until prebleach levels (within 0.1 log unit) were attained (12–14). For background adaptation, thresholds were measured at 12° inferior field dark-adapted or on an achromatic background that varied over −3.3 to +2.2 log scot.td range. Thresholds for two wavelengths (500, 650 nm) were determined to allow identification of the rod or cone mechanism mediating detection (11, 12). Threshold intensities are reported relative to an absolute standard (0 log level) of 1.6×10^{-16} W entering an 8-mm pupil (12).

ERG: Standard Protocol. ERGs were performed (14).

ERG: Photoresponse Activation. The leading edge of ERGs in response to high energy chromatic stimuli was used to quantify the activation phase of rod and cone phototransduction (13–17). A protocol to isolate the rod photoreceptor response in the homozygote was designed with consideration of reports of prolonged recovery of the suprathreshold ERG after a single light flash in Oguchi disease (18–20). After >8 hr of dark adaptation, a single blue (Wratten 47A) stimulus (4.6 log scot.td.s equivalent to 5.5 log photoisomerizations per rod) was delivered. This was followed by a single red (Wratten 26) stimulus (3.7 log phot.td.s), photopically matched to the blue stimulus. In the homozygote, this stimulus produced a dark-adapted cone ERG that was digitally subtracted from the first blue response to determine the rod-isolated photoresponse. In the heterozygote and normal subjects, the protocol and rod isolation were as described (16). Red (Wratten 26) stimuli (2.2 to 4.1 log phot.td.s) on a rod-desensitizing background (3.2 log phot.td) were used to isolate cone photoresponses in all subjects. A physiology-based model (13–17) was fitted to the leading edges of rod- and cone-isolated photoresponses to quantify the activation kinetics. Rod and cone amplification coefficients (21) can be estimated from the reported photoresponse sensitivities (16).

ERG: Rod Bipolar Cell Activation. The rod-isolated ERG b-wave component to a 4.6 log scot.td.s blue flash was estimated by digitally subtracting both the cone component and the rod photoresponse model fitted to the leading edge of the a-wave (15, 22, 23). In the homozygote, the cone component was the photopically matched red response. In the heterozygote and normal subjects, the red response was a mixture of rods and cones, the rod component of which was estimated by a dimmer blue response scotopically matched to the red response. The derived rod-isolated b-wave was normalized by the maximum amplitude of the rod photoresponse.

ERG: Photoresponse Recovery. The kinetics of recovery of maximal photoresponse amplitude following a high energy stimulus was quantified with a double-flash paradigm in rods (24–28) and cones (29). To estimate recovery of the rod photoresponse, we used a conditioning flash followed by a probe flash (both blue, Wratten 47A, 4.6 log scot.td.s) separated by an interstimulus interval (ISI) of 7–300 sec. The cone component of the probe response was estimated and subtracted. The probe response was

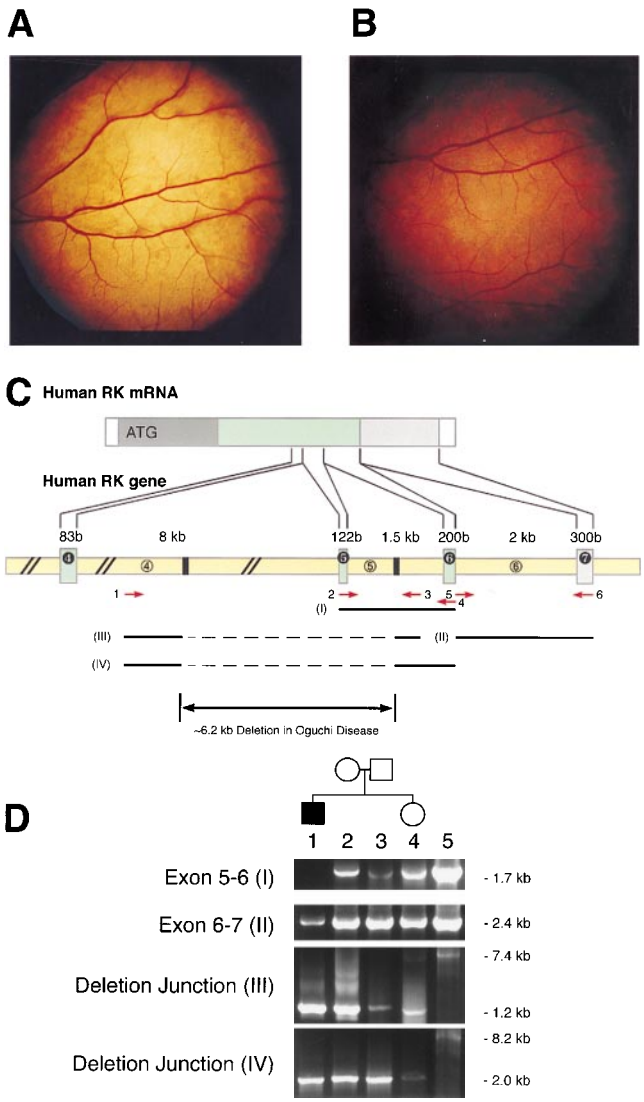

FIG. 1. Fundus photographs of the patient with Oguchi disease showing diagnostic metallic sheen in the light-adapted state (*A*) and disappearance of this abnormal sheen after 12 hr of dark-adaptation (*B*). (*C*) Structure of human RK mRNA (30, 31) and a partial structure of human RK gene including exons 4 to 7 (30). The arrows indicate the PCR primers used to analyze the RK gene; dashed line and double arrow indicate the deletion junction. (*D*) Agarose gel electrophoresis showing the PCR products from amplifying the genomic DNA of the patient (lane 1), his relatives (mother, lane 2; father, lane 3; sister, lane 4), and from the genomic clone encoding the normal RK gene (lane 5). Variability in the intensity of the bands between samples resulted from different extent of nonspecific hybridization of primers to genomic DNA.

fitted with the model of rod phototransduction and the fraction of maximum amplitude recovered was plotted against ISI. Recovery of the cone photoresponse was performed in the light-adapted state (3.2 log phot.td) with an achromatic conditioning stimulus (4.1 log phot.td.s) and a red (Wratten 26) probe stimulus (4.1 log phot.td.s). ISI was varied over 100–200 ms; several records (three or more in patients, two or more in normals) were obtained at each ISI. The probe response was fitted with the model of cone phototransduction and the model amplitude at 10 ms after the probe was plotted against ISI.

RESULTS

The patient, at age 4 years, was noted by his parents to be visually disabled in the dark but seemed fully sighted under well-lit conditions. No other family members had similar visual symptoms and there was no known parental consanguinity; both parents had Ashkenazi Jewish origins. On an examination at age 6, the patient had normal visual acuity and kinetic visual fields. A standard ERG revealed no detectable rod b-wave after 45 min of dark adaptation. A mixed cone-rod ERG to a bright flash of white light, dark-adapted, had an a-wave of normal amplitude but a reduced b-wave. Cone ERGs were normal. There was a metallic sheen to the retina (Fig. 1*A*); the coloration became normal after 12 hr of dark adaptation (Fig. 1*B*). The diagnosis was Oguchi disease. Eye examinations of the patient's mother and sister were normal. On reevaluation at age 13, the patient had normal thresholds on light-adapted static perimetry. Dark-adapted (>12 hr) perimetry showed rod threshold elevation (>2 SD from mean at each locus) at 30.5% of the loci tested (normal subjects average 1.7% of loci, range 0–6.9%). The threshold elevations at the patient's abnormal loci were between 0.5 and 1 log unit.

PCR using genomic DNA and specific primers that amplified fragments of the RK gene in the patient indicated a deletion of exon 5 (Fig. 1 *C* and *D*). All PCR fragments from the patient were cloned and sequenced, whereas those from his parents and an older female sibling were verified by restriction mapping and Southern blot analysis. Two primers within exon 5 and 6 (primers XZ-57 and XZ-54, respectively) were used to obtain a 1.7-kb fragment (product I) encompassing portion of exon 5 and 6 and the entire intron 5 from genomic DNA of the patient's relatives, and from a control genomic clone of human RK. No product was obtained from DNA of the patient, suggesting a deletion of exon 5 or 6 (Fig. 1). However, the 2.4-kb product II was obtained from all four family members based on primers encompassing a fragment of exon 6 and 7 (primers XZ-49 and XZ-46B), suggesting that exon 5, but not 6, is deleted from the gene encoding RK from the patient. Furthermore, two primers from intron 4 and 5 (XZ-59 and XZ-56) yielded 1.2-kb fragments (product III) instead of 7.4 kb, as detected by using the genomic clone. The DNA sequence of the 1.2-kb fragment revealed a deletion of exon 5, for which the patient is homozygous, whereas other family members are heterozygotes. Similarly, two primers located within intron 4 and exon 6 (XZ-59 and XZ-54), yielded 2.0-kb products (product IV) instead of the 8.2 kb as found by using DNA of the genomic clone. The lack of the 7.4- and 8.2-kb products from heterozygotes likely resulted from the difficulty of PCR amplification of these long fragments from complex human genomic DNA. The sequence of the deletion junction and the genomic clone showed that the patient has the same deletion of exon 5 in the RK gene as previously published (6). Analysis of exon 11 of the arrestin gene (5) showed no mutation (data not shown).

Based on the domain structure of RK, the allele containing the deletion will be "null" and functional RK is not produced (32). To further verify this prediction, human RK and RK lacking in exon 5 were expressed in COS-7 cells and assayed for the presence of immunoreactive protein and light-dependent phosphorylating activity with bovine rhodopsin as substrate. As seen from the immunoblot lane in Fig. 2*A*, 65- and 44-kDa bands corresponding to the wild-type and mutant proteins, respectively, are abundantly expressed in the COS-7 cell extracts transfected with pCMV-HRK and pCMV-HRK(X5 del). The molecular mass of these bands is consistent with predicted values based on the respective cDNA sequences. The mutant cDNA lacking in exon 5 sequence contains a premature termination codon and would be expected to encode a polypeptide chain of approximate M_r of 44,000 as opposed to a 65-kDa wild-type RK band, exactly as seen on the Western blots. To determine the activity of expressed proteins, supernatants of transfected COS-7 cells were assayed for light-dependent phosphorylating activity by using bovine rhodopsin as substrate. As seen in Fig. 2*B*, the extract from COS-7 cells transfected with pCMV-HRK plasmid encoding wild-type RK catalyzes incorporation of ^{32}P into a 40-kDa band corresponding to bovine rhodopsin only in the light (lane 2) but not the dark (lane 1) indicating presence of wild-type RK activity. The extracts from COS-7 cells transfected with the mutant plasmid pCMV-HRK(X5 del) fail to catalyze incorporation of ^{32}P into rhodopsin either in the light (lane 4) or in the dark (lane 3) indicating absence of all rhodopsin phosphorylating activity in the extract of COS cells expressing RK mutant lacking in exon 5.

Rod photoreceptor responses (Fig. 3*A*), representing the activation phase of phototransduction, had a maximum amplitude (354 μV) that was just within two SDs from mean normal (456 $\pm$ 54 μV, $n = 14$) for the homozygote and normal for the heterozygote (523 μV); the sensitivity parameter was normal in both patients (1.49 and 1.56 log scot.td^{-1}.s^{-3} for homozygote and heterozygote, respectively; normal = 1.52 $\pm$ 0.15 log scot.td^{-1}.s^{-3}, $n = 14$). For the derived rod b-wave (data not shown), normalized amplitude measured at the peak of the mean normal response (48 msec) was just within 2 SDs of normal (1.55 $\pm$ 0.30, $n = 14$) in the homozygote (1.0) and normal in the heterozygote (1.55). Cone photoresponse maximum amplitude (Fig. 3*B*) was normal (85 $\pm$ 9 μV, $n = 16$) in the homozygote (110 μV) and heterozygote (96 μV).

Recovery kinetics for rod-isolated photoresponses (Fig. 3 *C* and *E*) were abnormal in both homozygote and heterozygote. For

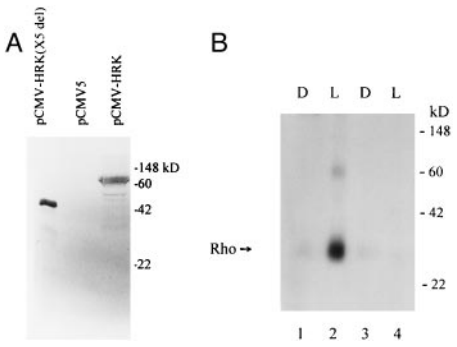

FIG. 2. Expression and activity of human RK and deletion of exon 5. (*A*) Immunoblots of extracts from COS-7 cells transfected with expression plasmids pCMV-HRK(X5 del), pCMV5, or pCMV-HRK. The COS-7 cell supernatants were electrophoresed on 10% SDS containing polyacrylamide gels and transferred to nitrocellulose membranes. The blots were developed by using alkaline phosphotase conjugated-secondary antibody after incubating the membranes with mouse mAbs against N-terminal domain of RK. (*B*) Autoradiogram showing relative incorporation of ^{32}P from ATP (100 μM, 2,000 dpm/pmol) into bovine rhodopsin (20 μM) catalyzed (at room temperature in the light or dark for 20 min) by extracts from COS-7 cells transfected with pCMV-HRK encoding wild-type RK (lanes 1 and 2) and pCMV-HRK(X5 del) encoding RK lacking in exon 5 (lanes 3 and 4). The positions of molecular mass markers and rhodopsin bands are indicated. The faint band seen in lane 2 probably represents rhodopsin dimer.

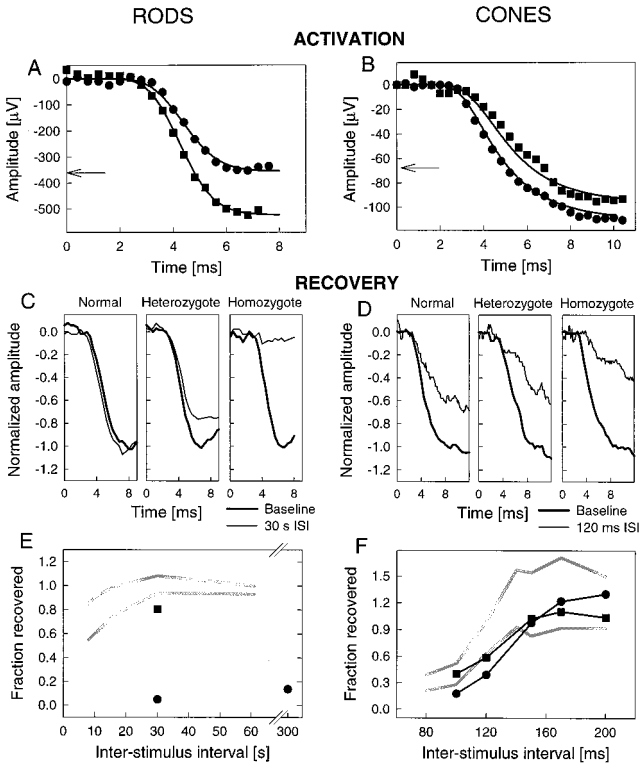

FIG. 3. Electrophysiological activation and recovery kinetics in rods and cones. Rod- (*A*) and cone-isolated (*B*) photoresponses representing activation in the homozygote (●) and heterozygote (■) evoked by 4.6 log scot.td.s blue (*A*) or 4.1 log phot.td.s. red stimuli (*B*). Lines show the fit to a model for activation of phototransduction. Arrows along the ordinate denote lower limit (mean − 2 SD) of photoresponse maximum amplitude. Recovery kinetics of rod- (*C*) and cone-isolated (*D*) photoresponses at a fixed ISI (30 sec in *C*, 120 msec in *D*) are shown for the patients and a representative normal subject. Baseline responses are thick lines and probe responses are thin lines. The fraction of baseline rod (*E*) and cone (*F*) photoresponse amplitudes that recovered for different ISIs in the homozygote (●), and heterozygote (■); gray lines represent the normal range.

the homozygote, the rod response probed 30 sec after the conditioning flash recovered to 5% of baseline maximum amplitude whereas normal subjects fully recover (range = 94%–108%, $n = 5$) in this interval. At 300 sec, the homozygote had recovered to 14% of baseline. The rod photoresponses in the heterozygote recovered to 81% of baseline in 30 sec. Recovery kinetics of cone-isolated photoresponses (Fig. 3 *D* and *F*) were normal in the heterozygote. The homozygote, however, showed a subtle but definite abnormality at ISIs of 100 msec (17.5%; normal range = 28–52%, $n = 5$) and 120 msec (39%; normal range = 63–99%, $n = 5$). The entire cone recovery curve of the homozygote appeared shifted to longer ISIs.

The kinetics of psychophysically measured rod dark adaptation after a 2% or 99% bleach had a dramatically slowed time course in the homozygote (Fig. 4*A*) but were normal in the heterozygote (Fig. 4*C*). In normal subjects, dark adaptation after small bleaches shows three linear components of rod-mediated recovery on a log-linear plot; after large bleaches, the first component is masked by initial cone-mediated recovery and only the second and third components are visible (12, 14, 33). In the homozygote, 2% and 99% bleaches showed cone-mediated recovery and a cone plateau followed by a rod-mediated linear component during which most of the measurable dynamic range of the rod system recovered; the last 0.5 log unit of sensitivity recovered at a slower rate. The major component of rod recovery in the homozygote had a slope of -0.03 log units.min^{-1} (time constant, 870 sec) that was ≈9 times slower than the normal second

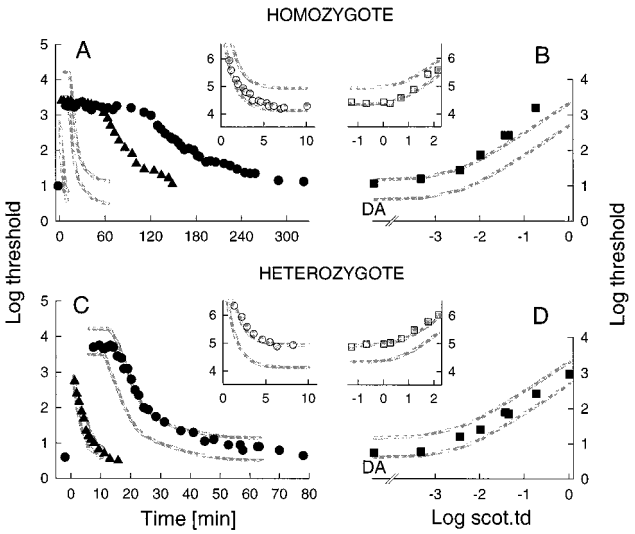

FIG. 4. Psychophysical bleaching and background adaptation. Dark adaptation after 2% (▲) or 99% (●) bleaches in the homozygote (*A*) and the heterozygote (*C*). Cone dark adaptation following 99% bleach shown in insets (◎). Rod-mediated (■) background adaptation in the homozygote (*B*) and the heterozygote (*D*). Cone mediated background adaptation shown in insets (▨). All main panels show thresholds to 500 nm stimuli (solid symbols) and all insets to 650 nm stimuli (gray symbols). Gray lines represent the normal range ($n = 12$ for bleaching, $n = 5$ for background adaptation). DA is dark-adapted. Prebleach thresholds are shown preceding time 0 in *A* and *C*. The horizontal axes of insets in *B* and *D* are in log phot.td. units.

component (normal range = -0.23 to -0.33 log units.min^{-1}, $n = 12$), but only slightly slower than the normal third component of recovery (range = -0.035 to -0.045 log units.min^{-1}, $n = 12$). The time for the rod system threshold to decrease below that of the cone system (rod-cone break) was prolonged to 120 min after a 99% bleach in the homozygote (normal mean = 12.5 ± 0.9 min, $n = 12$). Cone dark adaptation following a 99% bleach was normal in both subjects (Fig. 4 *A* and *C Insets*). The borderline thresholds of the heterozygote measured with 650 nm could be explained by her coincidental carrier state of an X-linked color defect, which the homozygote did not inherit.

In the homozygote, rod mediated increment thresholds were normal at low backgrounds (Fig. 4*B*). Starting at backgrounds of ≈−2.0 log scot.td., rod system adaptation became abnormal; the amount of abnormality increased with higher backgrounds. Cone mediated increment thresholds (Fig. 4*B Inset*) were normal in the homozygote. Both rod (Fig. 4*D*) and cone (Fig. 4*D Inset*) increment thresholds of the heterozygote were normal.

DISCUSSION

Analysis of Phenotype in a Known Oguchi Genotype. Oguchi disease, considered for decades to be caused by a postreceptor retinal defect like other retinopathies categorized as congenital stationary night blindness (34), has now been found to result from mutations in genes encoding proteins involved in photoreceptor function (5, 6). The current prospective analysis of the phenotype in Oguchi disease caused by a homozygous null mutation in the RK gene shows that the major abnormalities in disease expression could be localized to rod and cone photoreceptors and, specifically, to the process of recovery after light exposure.

Rod-isolated ERG photoresponses in the homozygote, although normal in phototransduction activation, showed a pronounced disturbance in recovery phase kinetics. Dark adaptation experiments showed that after partial and full bleaches rod-mediated thresholds did return to normal levels, but the dynamics of the recovery process were markedly

abnormal. A less dramatic but interesting result was that a relatively large number of loci in the visual field had abnormally elevated rod thresholds, even after dark adaptation for 12 hr. This finding, taken together with the borderline maximal amplitudes for the rod photoresponse and rod bipolar cell activity, could result from a small degree of persistent desensitization from incomplete dark adaptation. An alternative hypothesis is that rod cell abnormalities such as reduced outer segments or cell loss (35) are being detected by these methods. In the heterozygote, a small but significant rod photoreceptor recovery phase abnormality was detected, but other rod function measurements were normal. In the homozygote, light adaptation of the rod system was normal at low backgrounds but became increasingly abnormal at higher backgrounds. Cone-isolated ERG photoresponses of the homozygote were normal in phototransduction activation but showed a subtle disturbance in recovery phase kinetics. Cone-mediated recovery after a full bleach as well as light adaptation of the cone system were normal for both homozygote and heterozygote.

What is the Relationship of the Present Results to Previous Descriptions of Phenotype in Oguchi Disease of Known or Unknown Genotype? Of the three unrelated cases of Oguchi disease recently reported to have RK gene mutations (6), two patients were studied in detail with visual function tests ≈30 years ago (18, 36). Both a homozygote with an exon 5 deletion and a compound heterozygote with Val-380/Asp and Ser-536 (4-bp del) mutations had prolonged dark adaptation; the former had a slightly elevated dark-adapted threshold, even after 24 hr (18). Standard ERGs in the patient with an exon 5 deletion had a normal a-wave amplitude after extended dark adaptation but reduced amplitude after 10 min in the dark. Retinal densitometry in the compound heterozygote indicated rhodopsin kinetics were normal. Cone adaptometry and ERGs were mainly normal. The present work thus confirms and extends earlier studies.

In Japanese Oguchi patients with an arrestin gene mutation (1-bp deletion in codon 309 causing a frameshift and premature termination, ref. 5), there is a reduced standard ERG a-wave after 30 min of dark adaptation. Cone ERG, visual field, and visual acuity abnormalities were noted in some patients (37).

Oguchi patients of unknown genotype have shown prolonged or unmeasurable rod dark adaptation (38, 39) and rod ERG b-wave losses (4, 19, 39, 40). Some studies report reduced rod a-waves (38, 40, 41). Persistent psychophysical rod threshold elevations of ≈0.5 log units, even after 24 hr of dark adaptation, have been reported (20, 39). Delayed cone dark adaptation, elevated cone thresholds, and cone ERG abnormalities also have been documented (20, 38). Whether these differences in phenotype can be related to differences in genotype awaits further study.

What is the Current Understanding of Inactivation Steps in the Rod Visual Cycle? A series of conformational changes of rhodopsin starting with light-dependent isomerization of the chromophore, 11-*cis*-retinal, result in Rho*, which can continuously activate the phototransduction cascade with high efficiency. Some studies suggest that other intermediates of the visual cycle like noncovalent complexes of opsin and all-trans-retinal (42–44) or free opsin (45) also can activate the cascade albeit with lower efficiencies. For rods to regain full sensitivity, all of these (and other) activating species need to be turned off. In reconstituted systems and *in vivo*, RK phosphorylates Rho* and thus attenuates its activity (e.g., ref. 46). RK also may phosphorylate opsin/all-trans-retinal complexes (43). Subsequently, the phosphorylated receptor binds a regulatory protein, arrestin, completely quenching the activation of transducin (47). Inhibition of RK leads to prolonged photoresponses in functionally intact gecko rod outer segments (48). These and many other observations have led to the hypothesis that RK is important for inactivation of Rho*.

Concurrent with these inactivation steps, the photolyzed chromophore, all-trans-retinal, is removed (or just simply dissociates) from the binding site of rhodopsin and is reduced to all-trans-retinol by retinol dehydrogenase (3). The reduced chromophore, through a series of enzymatic steps in retinal pigment epithelium cells, is converted to 11-*cis*-retinal, which combines with opsin to regenerate rhodopsin. How both Rho* phosphorylation/arrestin binding and reduction of the chromophore contribute *in vivo* to the inactivation is uncertain. The inactivation processes are further complicated by the expression of a splice variant of arrestin that has significant affinity to unphosphorylated Rho* (49). It is possible that these three processes are decoupled from each other, independently reducing the catalytic power of Rho* and other activating intermediates.

How Do our Human *In Vivo* Results Relate to the Role of RK in Rods? From the rod-isolated photoresponse recovery experiments and rod bleaching adaptation data in the Oguchi patient, it is evident that rods do recover without RK, albeit much more slowly. A presumed role for RK in man, then, is to speed up the recovery of sensitivity in rods. Thirty seconds after a conditioning flash (0.4% rhodopsin bleach) that saturates the rods, no more than 5% of the dark current is reestablished in the patient whereas the dark current fully recovers in normal subjects. Upon more intense bleaching, the rod system in normals is desensitized for relatively long periods of time with full recovery of prebleach sensitivity occurring in 15 min (2% bleach) and 60 min (99%). Lack of RK increases the times to 60 min and >300 min, respectively. Recovery of sensitivity in the absence of RK can be speculated to occur by the reduction/regeneration cycle of the visual pigment, which would be a much slower process than the normal combination of phosphorylation and regeneration.

The exact cellular and molecular mechanisms underlying psychophysically determined bleaching adaptation remain speculative (33, 50). In normal subjects after a significant bleach, most of the psychophysically measurable dynamic range of rod-mediated vision recovers with an invariant time constant of ≈100 sec (12, 14, 33). Without functional RK, the time constant of the recovery increases to ≈900 sec. Also, in the homozygote, the initial desensitization caused by the major component of rod recovery, extrapolated to time zero (12, 33), is linearly related to bleach level. This suggests involvement of one of the earlier bleach products. Based on these data, we speculate that the second component (33) of recovery in normal bleaching adaptation represents the rate of phosphorylation of Rho* and opsin/all-trans-retinal complex, a reaction presumed to be missing in the homozygote. The approximate rate of phosphorylation determined *in vivo* during the first 2.5 min after a 45% bleach is consistent with this speculation (46). The rate of recovery observed in the homozygote, on the other hand, suggests that the rate of reduction of all-trans-retinal and dissociation of opsin may be approximately a first order reaction with a time constant of 900 sec. Of interest, the third component in normal bleaching adaptation that has been speculated to represent rhodopsin regeneration (33, 51) has a similar time constant (14, 33). It is possible that intracellular calcium-mediated feedback (52–54) turns RK activity off during the final log unit of recovery in the normal, thus slowing the recovery rate to approximate that of the Oguchi patient. This hypothesis is also consistent with the background adaptation abnormalities seen in the homozygote. At low intensity backgrounds thresholds are normal, but at higher backgrounds thresholds become increasingly abnormal possibly because at these background levels phosphorylation is turned on in normal subjects but not in the patient.

Based on data from transgenic mice in which a fraction of the rhodopsin molecules lacked the C terminus phosphorylation sites, it has been suggested that rhodopsin shutoff does not affect transducin activation during the early rising phase of single photon responses (55). Our results showing the activa-

tion steps of rod phototransduction to be indistinguishable in the presence or absence of RK are concordant.

Does RK Play a Role in Cone Deactivation? Light-activated species of cone pigments are believed to inactivate with processes similar to rods, but the kinetics are more rapid. The differences between rods and cones could result in part from a different subset of gene products involved in the inactivation of cone pigments (e.g., 56). RK may represent an exception; a cone-specific kinase has not been identified. Molecular cloning and immunolocalization studies have shown that both rod and cone photoreceptors express the same photoreceptor kinase and only RK has been cloned from the cone-dominated chicken retina (X.Z. and K.P., unpublished data). The finding of an abnormality in cone deactivation kinetics in the Oguchi patient suggests that RK plays a subtle role in cone recovery from light. The principle mechanisms of cone inactivation may be regeneration of cone pigment (2). This hypothesis is consistent with the normal bleaching adaptation found after a 99% cone bleach in the Oguchi patient. If true, this hypothesis suggests that isolated cone photoreceptor cell studies may be lacking the important and fast contribution of pigment regeneration to the recovery phase after light stimulation.

In summary, the lack of RK, resulting from a recessive human disease caused by a null mutation in the RK gene, causes a profound abnormality in recovery of rod photoreceptor function after light activation; and physiological evidence is provided that RK also may be involved in cone deactivation kinetics. This observation should be confirmed and extended by studying cone deactivation kinetics in other Oguchi patients with RK mutations and the results compared with those in patients with Oguchi disease caused by mutations in the arrestin gene that is believed to be rod-receptor specific. It also will be important to compare these human data with results from isolated rods and cones in animals with targeted deletion of the RK gene to gain detailed insights into the role RK plays in the subtle balance between inactivation and regeneration of visual pigment as the quiescent state of the photoreceptor is restored.

We thank Drs. T. D. Lamb and E. N. Pugh, Jr., for critical comments; Dr. E. Banin and Mr. Y. Huang for help with recordings and analyses; and Mr. M. Benegas and Mr. D. Hanna for clinical coordination. The work was supported by grants from the National Institutes of Health (EY08061, to K.P.; EY05627, to S.G.J. and A.V.C.; EY01730, to the University of Washington; EY01583, to the University of Pennsylvania); Foundation Fighting Blindness (to S.G.J. and A.V.C.); Whitaker Foundation (A.V.C.); Fight for Sight, Inc. (S.C.K.); and Research to Prevent Blindness, Inc. K.P. is a recipient of a Jules and Doris Stein Professorship from Research to Prevent Blindness.

1. Polans, A., Baehr, W. & Palczewski, K. (1996) *Trends Neurosci.* **19,** 547–554.
2. Smith, V. C., Pokorny, J. & Van Norren, D. (1983) *Vision Res.* **23,** 517–524.
3. Palczewski, K. & Saari, J. (1997) *Curr. Opin. Neurobiol.* **7,** 500–504.
4. Carr, R. E. (1991) in *Principles and Practice of Clinical Electrophysiology of Vision*, eds. Heckenlively, J. R. & Arden, G. B. (Mosby-Year Book, St. Louis), pp. 713–720.
5. Fuchs, S., Nakazawa, M., Maw, M., Tamai, M., Oguchi, Y. & Gal, A. (1995) *Nat. Genet.* **10,** 360–362.
6. Yamamoto, S., Sippel, K. C., Berson, E. L. & Dryja, T. P. (1997) *Nat. Genet.* **15,** 175–178.
7. Palczewski, K. (1997) *Eur. J. Biochem.* **248,** 261–269.
8. Premont, R. T., Macrae, A. D., Stoffel, R. H., Chung, N., Pitcher, J. A., Ambrose, C., Inglese, J., MacDonald, M. E. & Lefkowitz, R. J. (1996) *J. Biol. Chem.* **271,** 6403–6410.
9. Andersson, S., Davis, D. L., Dahlback, H., Jornvall, H. & Russell, D. W. (1989) *J. Biol. Chem.* **264,** 8222–8229.
10. Palczewski, K., Buczylko, J., Lebioda, L., Crabb, J. W. & Polans, A. S. (1993) *J. Biol. Chem.* **268,** 6004–6013.
11. Jacobson, S. G., Voigt, W. J., Parel, J.-M., Nghiem-Phu, L., Myers, S. W. & Patella, V. M. (1986) *Ophthalmology* **93,** 1604–1611.
12. Cideciyan, A. V., Lamb, T. D., Pugh, E. N., Jr., Huang, Y. & Jacobson, S. G. (1997) *Invest. Ophthalmol. Visual Sci.* **38,** 1786–1794.
13. Jacobson, S. G., Kemp, C. M., Cideciyan, A. V., Macke, J. P., Sung, C.-H. & Nathans, J. (1994) *Invest. Ophthalmol. Visual Sci.* **35,** 2521–2534.
14. Jacobson, S. G., Cideciyan, A. V., Kemp, C. M., Sheffield, V. C. & Stone, E. M. (1996) *Invest. Ophthalmol. Visual Sci.* **37,** 1662–1674.
15. Cideciyan, A. V. & Jacobson, S. G. (1993) *Invest. Ophthalmol. Visual Sci.* **34,** 3253–3263.
16. Cideciyan, A. V. & Jacobson, S. G. (1996) *Vision Res.* **36,** 2609–2621.
17. Jacobson, S. G., Cideciyan, A. V., Maguire, A. M., Bennett, J., Sheffield, V. C. & Stone, E. M. (1996) *Exp. Eye Res.* **63,** 603–608.
18. Carr, R. E. & Gouras, P. (1965) *Arch. Ophthalmol.* **73,** 646–656.
19. Gouras, P. (1970) *Invest. Ophthalmol.* **9,** 557–569.
20. Sharp, D. M., Arden, G. B., Kemp, C. M., Hogg, C. R. & Bird, A. C. (1990) *Clin. Vision Sci.* **5,** 217–230.
21. Pugh, E. N., Jr., & Lamb, T. D. (1993) *Biochim. Biophys. Acta* **1141,** 111–149.
22. Hood, D. C. & Birch, D. G. (1992) *Visual Neurosci.* **8,** 107–126.
23. Hood, D. C. & Birch, D. G. (1996) *J. Opt. Soc. Am. A* **13,** 623–633.
24. Birch, D. G, Hood, D. C., Nusinowitz, S. & Pepperberg, D. R. (1995) *Invest. Ophthalmol. Visual Sci.* **36,** 1603–1614.
25. Pepperberg, D. R., Birch, D. G., Hofmann, K. P. & Hood, D. C. (1996) *J. Opt. Soc. Am. A.* **13,** 586–600.
26. Hood, D. C., Cideciyan, A. V., Halevy, D. A. & Jacobson, S. G. (1996) *Vision Res.* **36,** 889–901.
27. Lyubarsky, A. L. & Pugh, E. N., Jr. (1996) *J. Neurosci.* **16,** 563–571.
28. Pepperberg, D. R., Birch, D. G. & Hood, D. C. (1997) *Visual Neurosci.* **14,** 73–82.
29. Hood, D. C., Birch, D. G. & Pepperberg, D. R. (1996) in *Vision Science and Its Applications,* OSA Technical Digest Series (Optical Soc. America, Washington, D.C.), Vol. 1, pp. 64–67.
30. Khani, S. C., Abitbol, M., Yamamoto, S., Maravic-Magovcevic, I. & Dryja, T. P. (1996) *Genomics* **35,** 571–576.
31. Zhao, X., Haeseleer, F., Fariss, R. N., Huang, J., Baehr, W., Milam, A. H. & Palczewski, K. (1997) *Visual Neurosci.* **14,** 225–232.
32. Zhao, X., Palczewski, K. & Ohguro, H. (1995) *Biophys. Chem.* **56,** 183–188.
33. Lamb, T. D. (1981) *Vision Res.* **21,** 1773–1782.
34. Berson, E. L. (1994) in *Principles and Practice of Ophthalmology*, eds. Albert, D. M. & Jakobiec, F. A. (Saunders, Philadelphia), pp. 1214–1237.
35. Shady, S., Hood, D. C. & Birch, D. G. (1995) *Invest. Ophthalmol. Visual Sci.* **36,** 1027–1037.
36. Carr, R. E. & Ripps, H. (1967) *Invest. Ophthalmol.* **6,** 426–436.
37. Nakazawa, M., Wada, Y., Fuchs, S., Gal, A. & Tamai, M. (1997) *Retina* **17,** 17–22.
38. Doesschate, J. T., Alpern, M., Lee, G. B. & Heyner, F. (1966) *Doc. Ophthalmol.* **20,** 406–419.
39. Krill, A. E. (1977) in *Krill's Hereditary Retinal and Choroidal Diseases*, ed. Krill, A. E. (Harper & Row, Hagerstown, MD), pp. 391–420.
40. Miyake, Y., Horiguchi, M., Suzuki, S., Kondo, M. & Tanikawa, A. (1996) *Jpn. J. Ophthalmol.* **40,** 511–519.
41. Kubota, Y. (1966) in *Retinal Degenerations, ERG and Optic Pathways*, ed. Nakamura, A. (Maruzen, Tokyo), pp. 317–324.
42. Jager, S., Palczewski, K. & Hofmann, K. P. (1996) *Biochemistry* **35,** 2901–2908.
43. Buczylko, J., Saari, J. C., Crouch, R. K. & Palczewski, K. (1996) *J. Biol. Chem.* **271,** 20621–20630.
44. Crouch, R. K., Chader, G. J., Wiggert, B. & Pepperberg, D. R. (1996) *Photochem. Photobiol.* **64,** 613–621.
45. Fain, G. L., Matthews, H. R. & Cornwall, M. C. (1996) *Trends Neurosci.* **19,** 502–507.
46. Ohguro, H., Van Hooser, J. P., Milam, A. H. & Palczewski, K. (1995) *J. Biol. Chem.* **270,** 14259–14262.
47. Wilden, U., Hall, S. W. & Kühn, H. (1986) *Proc. Natl. Acad. Sci. USA* **83,** 1174–1178.
48. Palczewski, K., Rispoli, G. & Detwiler, P. B. (1992) *Neuron* **8,** 117–126.
49. Palczewski, K., Buczylko, J., Ohguro, H., Annan, R. S., Carr, S. A., Crabb, J. W., Kaplan, M. W., Johnson, R. S. & Walsh, K. A. (1994) *Protein Sci.* **3,** 314–324.
50. Stabell, U. & Stabell, B. (1996) *Scand. J. Psychol.* **36,** 259–268.
51. Kemp, C. M., Jacobson, S. G., Cideciyan, A. V., Kimura, A. E., Sheffield, V. C. & Stone, E. M. (1994) *Invest. Ophthalmol. Visual Sci.* **35,** 3154–3162.
52. Kawamura, S. (1994) *Neurosci. Res.* **20,** 293–298.
53. Koutalos, Y. & Yau, K.-W. (1996) *Trends Neurosci.* **19,** 73–81.
54. Chen, C. K., Inglese, J., Lefkowitz, R. J. & Hurley, J. B. (1995) *J. Biol. Chem.* **270,** 18080–18066.
55. Chen, J., Makino, C. L., Peachey, N. S., Baylor, D. A. & Simon, M. I. (1995) *Science* **267,** 374–377.
56. Craft, C. M. & Whitmore, D. H. (1995) *FEBS Lett.* **362,** 247–255.